Article

Infrared-Visible Sum Frequency Generation Spectroscopic Study of Molecular Orientation at Polystyrene/Comb-Polymer Interfaces

Gary P. Harp, Hasnain Rangwalla, Mohsen S. Yeganeh, and Ali Dhinojwala

J. Am. Chem. Soc., **2003**, 125 (37), 11283-11290• DOI: 10.1021/ja035513v • Publication Date (Web): 20 August 2003

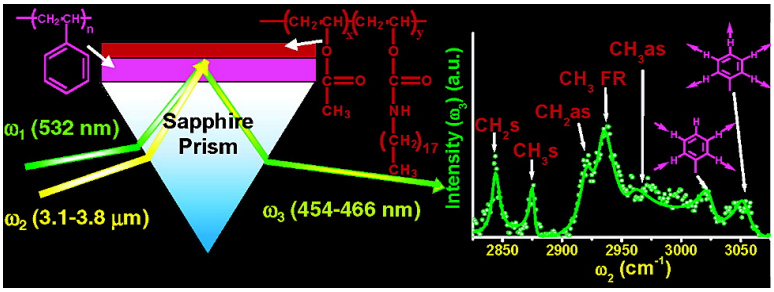

More About This Article

Additional resources and features associated with this article are available within the HTML version:

- Supporting Information
- Links to the 5 articles that cite this article, as of the time of this article download
- Access to high resolution figures
- Links to articles and content related to this article
- Copyright permission to reproduce figures and/or text from this article

View the Full Text HTML

J|A|C|S
ARTICLES
Published on Web 08/20/2003

Infrared-Visible Sum Frequency Generation Spectroscopic Study of Molecular Orientation at Polystyrene/Comb-Polymer Interfaces

Gary P. Harp,[†] Hasnain Rangwalla,[†] Mohsen S. Yeganeh,[‡] and Ali Dhinojwala*[,†]

Contribution from the Department of Polymer Science, The University of Akron, Akron, Ohio 44325, and ExxonMobil Research and Engineering Co., Annandale, New Jersey 08801

Received April 7, 2003; E-mail: alid@polymer.uakron.edu

Abstract: Surface-sensitive infrared−visible sum frequency generation spectroscopy (SFG) in total internal reflection geometry has been used to study the structure of poly(vinyl *n*-octadecyl carbamate-*co*-vinyl acetate) (PVNODC) or poly(octadecyl acrylate) (PA-18) in contact with a deuterated or hydrogenated polystyrene (dPS or hPS) layer. SFG spectra from the PVNODC (or PA-18)/hPS interface show methyl and methylene peaks corresponding to PVNODC (or PA-18) and phenyl peaks corresponding to the PS. Analysis suggests that the methyl groups are tilted at angles less than 30° with respect to the surface normal. The presence of a strong methylene peak suggests the PVNODC alkyl side chains contain more gauche defects at the PS/PVNODC interface in comparison to PVNODC (or PA-18)/air interfaces. On heating, the SFG intensity from the PS/PA-18 interface drops sharply near the bulk melting temperature (T_m) of PA-18. Interestingly, a similar drop in SFG signal is also observed for the PS phenyl groups. This demonstrates the ability of the phenyl group at the PS/PA-18 interface to rearrange itself upon the solid-to-liquid transition of the PA-18 alkyl side chain, at a temperature well below the bulk PS glass transition temperature. For PS/PVNODC interfaces, the drop in SFG intensity is gradual and in agreement with the three broad transitions of PVNODC observed in the bulk.

1. Introduction

The understanding of polymer/polymer interfaces is of considerable scientific and technological interest because of their widespread importance in adhesion, optical films, microelectronics, polymer blends, composites, and polymer light-emitting diodes. Controlling the interfacial energy, a quantity determined by the composition, orientation, and distribution of functional groups, is the common goal in these applications. In this work, we are interested in interfaces of alkyl side-chain polymers that are routinely used as release coatings for pressure-sensitive adhesives and in wax deposition inhibitors.[1−4] The long, hydrophobic side chains segregate to the air interface and provide a nonstick surface for good release. Consequently, the adhesion and wetting behavior is strongly influenced by the bulk side chain melting temperature.[1−3] A fact that has been exploited in the development of "smart" materials that exhibit different interfacial energy vis-à-vis different interfacial functionality that can be reversibly varied using temperature.[1] It has recently been shown that the room-temperature surface of these polymers consists of crystalline side chains in predominantly all-trans conformations.[5,6] This is reminiscent of well-ordered hydrocarbon chains observed in self-assembled monolayers. Although the structure of these release coatings at the air interface is now well understood, the structure in contact with a polymer, the interface of interest in practical applications, is poorly understood. It is expected that the presence of another polymer (or adhesive) at the interface will influence the structure and orientation of molecules in comparison to the structure and orientation observed at the air or vacuum interface. The conventional techniques used to study air or vacuum interfaces do not provide the information on orientation and structure of molecules at the hidden interface.

Recently, we have demonstrated that surface-sensitive infrared−visible sum frequency generation spectroscopy (SFG) in an internal reflection geometry can be used to directly probe the structure and orientation of molecules at polymer/polymer interfaces.[7] SFG involves spatially and temporally mixing a visible, high-intensity laser beam of frequency ω_1 with a tunable infrared wavelength source of frequency ω_2 at the interface of interest. According to the dipole approximation, generation of a SFG photon [at $(\omega_1 + \omega_2)$] is forbidden in the centrosymmetric

[†] The University of Akron.
[‡] ExxonMobil Research and Engineering Co. (mohsen.s.yeganeh@exxonmobil.com).

(1) De Crevoisier, G.; Fabre, P.; Cropart, J. M.; Leibler, L. *Science* **1999**, *285*, 1246−1250.
(2) Li, L.; Macosko, C.; Korba, G. L.; Pocius, A. V.; Tirrell, M. *J. Adhes.* **2001**, *77*, 95−123.
(3) Kinning, D. J. *J. Adhes.* **1997**, *60*, 249−274.
(4) Zeng, H. Y.; Zhang, W. B.; Li, Z. M. *J. Appl. Polym. Sci.* **1991**, *43*, 919−923.
(5) Gautam, K. S.; Dhinojwala, A. *Macromolecules* **2001**, *34* (5), 1137−1140.
(6) Gautam, K. S.; Dhinojwala, A. *Phys. Rev. Lett.* **2002**, *88*, 145501−1/5.
(7) Harp, G. P.; Gautam, K. S.; Dhinojwala, A. *J. Am. Chem. Soc.* **2002**, *124*, 7908−7909.

bulk and is nonzero at interfaces where inversion symmetry is broken. The SFG is resonantly enhanced when ω_2 overlaps with the resonant frequency of a molecular vibrational mode that is both infrared- and Raman-active. The SFG signals are also enhanced when the incidence angle of the input beams is close to the critical angle for the total internal reflection geometry, due to enhancement in Fresnel coefficients. We have used this enhancement in SFG signals to probe polymer/solid and polymer/polymer interfaces.[7,8] Other geometries to probe polymer/polymer interfaces by SFG have also been reported recently.[9,10] The application of SFG to study other interfaces has been discussed in several review articles recently.[11−13]

We report here SFG measurements on poly(vinyl octadecyl-carbamate-*co*-vinyl acetate) (PVNODC) and poly(octadecyl acrylate) (PA-18) in contact with hydrogenated or deuterated polystyrene (hPS or dPS). PVNODC is primarily composed of carbamate repeat units and PA-18 is composed entirely of acrylate repeat units; both of these repeat units have 18-carbon-long alkyl side chains. In a recent communication, we have shown that the SFG spectra at PS/PVNODC interfaces are different from spectra at polymer/air or polymer/sapphire interfaces.[7] Here, we present the complete analysis of the SFG spectra and changes in the structure on heating. We find that the alkyl side chains of PVNODC have significantly more gauche defects in comparison to the air interface and the terminal methyl groups are tilted less than 30° with respect to the surface normal, similar to the air interface. Further, the phenyl groups of the PS chains at the PS/PVNODC interface are tilted in comparison to those at the air interface.[8] On heating, we find an abrupt drop in SFG intensity at 43 °C for the PS/PA-18 interface coinciding with the bulk transition of PA-18, also at 43 °C. The drop in SFG intensity for the PVNODC/PS interface is gradual and matches with the broad transitions observed in bulk PVNODC. These observations indicate that the disordering is correlated with the bulk structure and transition temperatures. Interestingly, the phenyl SFG intensity decreases at the same temperatures as the methyl and methylene intensity of the PA-18 or PVNODC alkyl side chains, suggesting that the phenyl groups at the PS/PA-18 (or PVNODC) interface are able to rearrange in response to changes in the environment induced by the melting of the PA-18 or PVNODC side chains.

2. SFG Background

The geometry of the SFG measurements is shown in Figure 1. The media are labeled with their refractive indices n_i where the subscripted numbers $i = 0$, 1, 2, and 3 correspond to the air, sapphire prism, PS film, and PVNODC or PA-18 film, respectively (see Supporting Information for numerical values). The reflected output SFG intensity $I_3(\omega_3)$ from the PS/Comb-polymer interface between media 2 and 3 in Figure 1 can be expressed as a product of the square of the effective second-order nonlinear-susceptibility tensor $\chi_{\text{eff}}^{(2)}$ and the intensities of the input beams $I_i(\omega_i)$ in the following way:[14]

$$I_3(\omega_3) = \frac{8\pi^3 \omega_3^{\,2} \sec^2 \phi_D(\omega_3)}{c^3 n_2(\omega_3) n_2(\omega_2) n_2(\omega_1)} |\chi_{\text{eff}}^{(2)}|^2 I_1(\omega_1) I_2(\omega_2) \qquad (1)$$

where $\phi_D(\omega_3)$ is the output angle at the sum frequency ω_3 with respect to the interface normal (and is determined by the conservation of momentum parallel to the interface at the SFG frequency), and $n_2(\omega_i)$ are the refractive indices of medium 2 at ω_1, ω_2, and ω_3. The intensities of the visible and infrared laser beams, I_1 and I_2, are given by the following general form, where T^{kl} is a Fresnel factor describing reflection losses in transmission between two media k and l of different refractive index and E_i is the magnitude of the input electric field:[15]

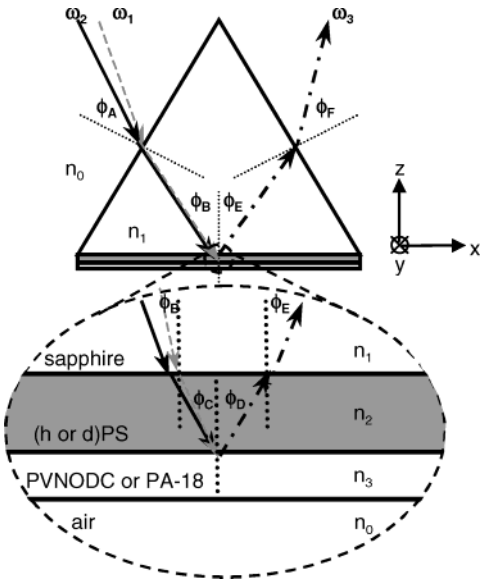

Figure 1. Schematic diagram of the 60° prism/polymer bilayer sample geometry for total internal reflection sum frequency generation: ω_1 is the input visible beam, ω_2 the input infrared, and ω_3 the reflected SFG beam. ϕ_i represents the input and output angles with respect to the interface normal for the various interfaces. The inset shows the four media involved in this sample geometry labeled by their refractive index n_i with the beam path to and from the polymer/polymer interface as well as the Cartesian axes (x, y, z) of the laboratory fixed coordinate system.

$$I_i(\omega_i) = \frac{c n_i(\omega_i)}{4\pi} |T^{12}(\omega_i) T^{01}(\omega_i) E_i(\omega_i)|^2 \qquad (2)$$

$\chi_{\text{eff},ijk}^{(2)}$ can be expressed as the sum of a constant nonresonant term of relative phase φ and the sum of resonant vibrations:

$$\chi_{\text{eff},ijk}^{(2)} = (\chi_{\text{f},ijk}^{\text{NR}} e^{i\varphi} + \sum_q \chi_{\text{q},ijk}^{\text{R}}) = \left(\chi_{\text{f},ijk}^{\text{NR}} e^{i\varphi} + \sum_q \frac{A_{q,ijk}}{\omega_2 - \omega_q - i\Gamma_q}\right) \qquad (3)$$

where A_q, Γ_q, and ω_q are the line strength, homogeneous line width, and resonant frequency of the qth vibration.

The resonant portion of the continuum nonlinear susceptibility can be related to the product of the number of molecules present at the interface, N, and the ensemble average of the sum of the molecular hyperpolarizability. This is determined by transformation of second-order molecular hyperpolarizabilities, β_{lmn}, from the molecular frame of reference (l, m, n) to the i, j, k (x, y, z) axes of the lab frame of reference (Figure 1 inset) as follows:

(8) Gautam, K. S.; Schwab, A. D.; Dhinojwala, A.; Zhang, D.; Dougal, S. M.; Yeganeh, M. S. *Phys. Rev. Lett.* **2000**, *85* (18), 3854−3857.
(9) Chen, C.; Wang, J.; Even, M. A.; Chen, Z. *Macromolecules* **2002**, *35*(21), 8093−8097.
(10) Liu, Y.; Messmer, M. C. *J. Am. Chem. Soc.* **2002**, *124*, 9714−9715.
(11) Miranda, P. B.; Shen, Y. R. *J. Phys. Chem. B* **1999**, *103*, 3292−3307.
(12) Chen, Z.; Shen, Y. R.; Somorjai, G. A. *Annu. Rev. Phys. Chem.* **2002**, *53*, 437−465.
(13) Buck, M.; Himmelhaus, M. *J. Vac. Sci. Technol. A.* **2001**, *19*(6), 2717−2736.
(14) Zhuang, X.; Miranda, P. B.; Kim, D.; Shen, Y. R. *Phys. Rev. B* **1999**, *59*(19), 12632−12640.
(15) Born, M.; Wolf, E. *Principles of Optics*, 7th ed.; Cambridge University Press: Cambridge, U.K., 1999; Chapter 2.

$$\chi_{q,ijk}{}^{R} = N\int[\sum_{lmn} U_{ijk,lmn}\beta_{lmn}]f(\Omega)\,d\Omega \quad (4)$$

Ω represents the Euler angles (θ, χ, ϕ) that relate the two coordinate systems. $U_{ijk,lmn}$ are Euler transformation coefficients and have been tabulated by Hirose et al.,[16] and $f(\Omega)$ is the orientational probability distribution function. The hyperpolarizability tensor β_{abc} for a single molecule is the product of the *ab* component of the Raman tensor, $d\alpha_{ab}/dq$, and the *c* component of the infrared dipole moment derivative, $d\mu_c/dq$. As a consequence, a vibrational mode must be both infrared- and Raman-active in order to be SFG-active.

For the interfaces between the thin films of PS and PVNODC or PA-18 in the experimental geometry described in Figure 1, the plane of the interface is azimuthally isotropic, leaving only 4 of 27 independent components $\chi_{q,ijk}{}^{R}$ of the $\chi_q{}^{R}$ tensor.[14] By choosing polarization combinations, selected components or combinations of these components may be probed. In this paper, SSP and SPS are the two polarization combinations of interest, where S and P refer to light polarized in the plane of the interface and normal to the plane of the interface, respectively. The polarization combinations above are given in the following sequence: polarization of the SFG beam, visible beam, and infrared beam. Expressions for these combinations are given below.[14]

$$\chi_{eff,SSP}{}^{(2)} = L_{yy}(\omega_3)L_{yy}(\omega_1)L_{zz}(\omega_2)\sin\phi_D(\omega_2)\chi_{eff,yyz}{}^{(2)}$$
$$\chi_{eff,SPS}{}^{(2)} = L_{yy}(\omega_3)L_{zz}(\omega_1)L_{yy}(\omega_2)\sin\phi_D(\omega_1)\chi_{eff,yzy}{}^{(2)} \quad (5)$$

The angles $\phi_D(\omega_2)$ and $\phi_D(\omega_1)$ are the input angles of the respective visible and infrared beams relative to the interface normal depicted in Figure 1, and the L_{ij} are Fresnel factors[15] that describe the interfacial electric fields. These Fresnel factors are determined by incident and transmission angles of the input and the SFG beams, respectively. Thus, judicious choice of the input angles ϕ_A (ω_2) and ϕ_A (ω_1) at the face of the prism allows us to selectively enhance $\chi_{eff}{}^{(2)}$ at the polymer/solid, polymer/polymer, or polymer/air interfaces.[6−8]

Vibration bands of the three functional groups, methyl, methylene, and phenyl, are observed in the SFG spectra at the polymer/polymer interface. The relevant normal modes of vibration for these groups are depicted in their respective *l, m, n* (*a, b, c*) Cartesian coordinates of molecular hyperpolarizability shown in Figure 2A. The transformation coefficients $U_{lmn,ijk}$ as determined by Hirose et al.[16] and the assumption of a random isotropic distribution of the angles ϕ and χ were used to determine the expressions relating $\chi_{eff,ijk}$ and tilt angle θ, which describes the tilt of the molecular symmetry axis *c* from the interface normal *z*. Expressions given below for the methyl modes are based on the hyperpolarizability components for a molecule of C_{3v} symmetry and are those of Hirose.[17]

For methyl r^+ mode:

$$\chi_{yyz}{}^{(2)} = -N\left\{\left(\frac{\beta_{aac}-\beta_{ccc}}{2}\right)[\langle\cos\theta\rangle - \langle\cos^3\theta\rangle] - \beta_{aac}\langle\cos\theta\rangle\right\} \quad (6)$$

$$\chi_{yzy}{}^{(2)} = -N\left\{\left(\frac{\beta_{aac}-\beta_{ccc}}{2}\right)[\langle\cos\theta\rangle - \langle\cos^3\theta\rangle]\right\} \quad (7)$$

For methyl r^- mode:

$$\chi_{yyz}{}^{(2)} = -N\beta_{aca}[\langle\cos\theta\rangle - \langle\cos^3\theta\rangle] \quad (8)$$

$$\chi_{yzy}{}^{(2)} = N\beta_{aca}\langle\cos^3\theta\rangle \quad (9)$$

Both methylene and phenyl groups are of C_{2v} symmetry, and transformations assuming an isotropic random distribution of angles around

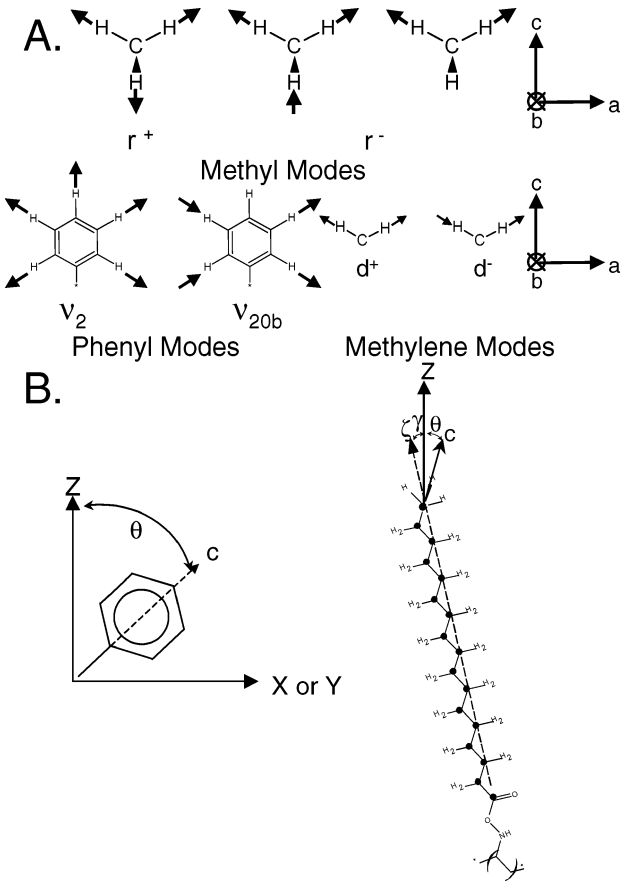

Figure 2. (A) Normal modes of vibration for the methyl, methylene, and phenyl groups observed in SFG spectra and the Cartesian coordinates of their respective molecule fixed hyperpolarizability. (B) Schematic planar projections of an all-trans PVNODC alkyl side chain and a phenyl group illustrating the definition of θ: the tilt angle between the *c*-axis of the molecule-fixed coordinate system and the *z* axis of the laboratory-fixed coordinate system. The PVNODC side-chain axis *w* and tilt angle ζ are also labeled.

ϕ and χ are provided below for vibrations of the symmetric and asymmetric irreducible representations.

For the phenyl ν_2 mode:

$$\chi_{yyz}{}^{(2)} = N\left\{\left(\frac{\beta_{aac}}{2}\right)\langle\cos\theta\rangle + \left(\frac{\beta_{aac}-2\beta_{ccc}}{16}\right)[\langle\cos 3\theta\rangle - \langle\cos\theta\rangle]\right\} \quad (10)$$

$$\chi_{yzy}{}^{(2)} = N\left(\frac{\beta_{aca}}{8}\right)[\langle\cos 3\theta\rangle - \langle\cos\theta\rangle] \quad (11)$$

For the phenyl ν_{20b} mode:

$$\chi_{yyz}{}^{(2)} = N\left(\frac{\beta_{aac}-2\beta_{ccc}}{16}\right)[\langle\cos 3\theta\rangle - \langle\cos\theta\rangle] \quad (12)$$

$$\chi_{yzy}{}^{(2)} = N\left\{\left(\frac{\beta_{aca}}{2}\right)\langle\cos\theta\rangle + \left(\frac{\beta_{aca}}{8}\right)[\langle\cos 3\theta\rangle - \langle\cos\theta\rangle]\right\} \quad (13)$$

The assumption of an isotropic random distribution of angles around ϕ and χ leaves only the θ component of $f(\Omega)$, and the relevant ensemble averages are defined as follows:

(16) Hirose, C.; Akamatsu, N.; Domen, K. *Appl. Spectrosc.* **1992**, *46* (6), 1051−1072.
(17) Watanabe, N.; Yamamoto, H.; Wada, A.; Akamatsu, N.; Hirose, C.; Ohtake, T.; Norihisa, M. *Spectrochim. Acta* **1994**, *50* (8/9), 2529−1537.

$$\langle \cos\theta \rangle = K\int_{-\infty}^{+\infty} \cos(\theta)P(\theta)\sin\theta\, d\theta$$

$$\langle \cos 3\theta \rangle = K\int_{-\infty}^{+\infty} \cos(3\theta)P(\theta)\sin\theta\, d\theta$$

$$K = [\int_{-\infty}^{+\infty} P(\theta)\sin\theta\, d\theta]^{-1} \quad (14)$$

where $P(\theta)$ is a Gaussian function, with a width σ and peak at θ_0:

$$P(\theta) = \frac{1}{\sigma\sqrt{\pi/2}} e^{[-2(\theta-\theta_0)^2/\sigma^2]} \quad (15)$$

3. Experimental Section

A. Sample Preparation and Peel Testing. Hydrogenated (M_w = 108 kg/mol, $M_w/M_n \approx 1.08$) and deuterated (M_w = 125 kg/mol, $M_w/M_n \approx 1.13$) poly(styrenes) were purchased from Polymer Source. PVNODC [poly(vinyl-*n*-octadecylcarbamate-*co*-vinyl acetate) (M_w = 70 kg/mol, $M_w/M_n \approx 3.0$)] and PA-18 [poly(octadecyl acrylate) (M_w = 65 kg/mol, $M_w/M_n \approx 3.5$)] were obtained as gifts from 3M Corporation and Scientific Polymer Products Inc., respectively. Samples were prepared by spin-coating a film ~300 nm thick from a 5 wt % solution of hPS or dPS in toluene onto the surface of a 60° sapphire prism. The film was then annealed under vacuum for 3 h at 110 °C. A second film ~200 nm thick was then spin-cast on top of the first from a warm 6 wt % solution of PVNODC or PA-18 in a 50/50 mixture of octanol and *n*-butanol (both nonsolvents for PS). The bilayer sample was then annealed again at 110 °C in a vacuum for 3 h. Samples were allowed to cool slowly to room temperature before use. A Tencor Alpha-Step profilometer was used to measure the film thickness.

To provide a qualitative measure of adhesive behavior, a simple crosshatch adhesion test, similar to typical paint and coating peel tests, was performed with commercial pressure-sensitive adhesive tape on bilayer samples prepared as above. The bilayer samples were given a brief ~1 s oxygen plasma treatment with a Harrick PDC-32G plasma cleaner set on high to allow the tape to adhere to the top PVNODC layer and scored into a horizontal 4 × 4 grid. Adhesive tape was pressed into contact with the upper PVNODC layer and then peeled off, and the interface of failure for each square was determined on the basis of the absence or presence of the thin film interference color of the polystyrene film.

B. SFG Measurements. SFG experiments with narrow wavenumber resolution were performed at the ExxonMobil SFG system II. Infrared pulses (1−2 mJ, 0.2 cm^{-1} bandwidth, ~15 ns pulse duration, 10 Hz repetition rate), tunable from 2750 to 3200 cm^{-1}, and visible pulses (3 mJ, 0.2 cm^{-1}, 10 Hz) were overlapped at the polymer-coated face of sapphire prism (optic axis passing through the center of the prism and parallel to the face of the prism with a tolerance of ±2°) at an incident angle of ~8° with respect to the face of the prism. SFG signals are normalized with the output energy of the visible laser and the infrared energy measured just prior to the sample. We have verified that at these incident angles the SFG signals are dominated by the interface between the two polymers.[7] The details of the laser set up are discussed elsewhere.[18]

The temperature dependence measurements were performed on the Spectra-Physics laser system at the University of Akron with a tunable infrared output (2700−3200 cm^{-1}, 1 ps pulse width, 1 kHz repetition rates, and fwhm ~ 20 cm^{-1}) overlapped with an 800 nm visible output (1 ps pulse width and 1 kHz repetition rates). Output SFG signal was passed through interference filters and measured by use of a photomultiplier tube. Data were collected at 5 cm^{-1} intervals. The prism was mounted on a custom-designed heating cell, and temperature was varied via a Lakeshore Cryotronics 331 temperature controller. The constant-heating and constant-cooling rate measurements were taken during the second heating and cooling cycles to remove any influence of prior thermal history. Isothermal SFG spectra were taken after the sample temperature stabilized to within less than ±0.5 °C.

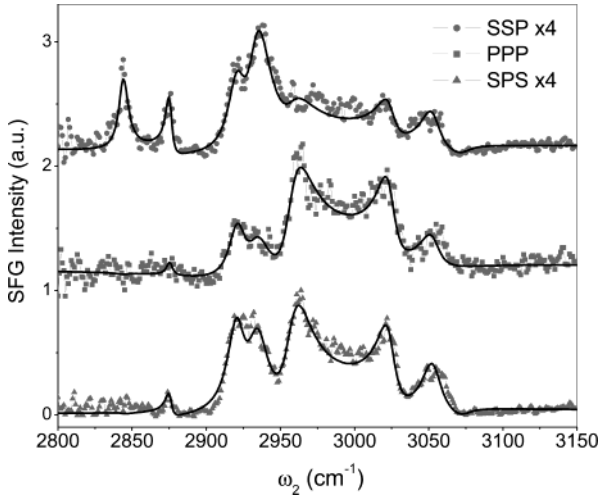

Figure 3. SFG spectra from the hPS/PVNODC interface at an incident angle $\phi_A \approx 8°$ at three different polarization conditions SSP, PPP, and SPS. The SSP and SPS spectra are scaled by a factor of 4 and are offset for presentation. The solid lines are fits to the square of the sum of Lorentzian functions describing the resonant peaks and a nonresonant background (eq 3).

C. Differential Scanning Calorimetry. Differential scanning calorimetry was performed on a TA Instruments DSC 2910 equipped with a liquid nitrogen cooling accessory at heating and cooling rates of 0.5 °C/min. Reported scans are for the second heat and second cool, after one complete heating and cooling cycle.

4. Results and Discussion

We have divided this section into three parts. In section A, we analyze the orientation of methyl, methylene, and phenyl groups based on SFG spectra at room temperature and discuss the determined group orientation with respect to the observed adhesive behavior of the interface. In section B, we discuss the spectral changes with temperature and the relationship between the interfacial and bulk transition temperatures with regard to the possible interfacial structures. In section C, we discuss the consequences of the interfacial structure on the release properties of PVNODC.

A. Static Measurements of the PS/PVNODC Interface. Figure 3 shows SFG spectra in the SSP, SPS, and PPP polarization for the hPS/PVNODC interface. The methyl and methylene groups give rise to five C−H stretching vibrational modes, depicted in Figure 2A, and one Fermi resonance combination band at wavenumbers between 2800 and 3000 cm^{-1}. The vibrational modes r^+ methyl symmetric, r^- methyl asymmetric, r^{FR} methyl symmetric Fermi resonance, d^+ methylene symmetric, and d^- methylene asymmetric are assigned to bands at 2875, 2960, 2935, 2845, and 2918 cm^{-1}, respectively.[19] In Figure 3, the symmetric methyl r^+ and symmetric methylene d^+ vibration bands are clearly resolved in the SSP spectra and the r^- asymmetric methyl band dominates the SPS and PPP spectra. The d^- and r^{FR} vibrational bands are also clearly resolved in the SSP, SPS, and PPP spectra in Figure 3. Comparison of spectra from the dPS/PVNODC and the hPS/PVNODC interface discussed in part B and in our previous

(18) Yeganeh, M. S.; Dougal, S. M.; Poilizzotti, R. S.; Rabinowitz, P. *Thin Solid Films* **1995**, *270*, 226−230.

(19) MacPhail, R. A.; Strauss, H. L.; Snyder, R. G.; Elliger, C. A. *J. Phys. Chem.* **1984**, *88*, 334−341.

communication[7] are similar below 3000 cm^{-1}. This indicates that these five methyl and methylene vibrations are from PVNODC segments and not PS, since dPS has no vibrational assignments in the 2800−3200 cm^{-1} range.

The presence of all five methyl and methylene vibration bands in the SSP spectra from the hPS (or dPS)/PVNODC interfaces is in sharp contrast to SSP spectra for the PVNODC/air and sapphire/PVNODC interfaces of a solitary PVNODC film measured previously.[7] In the SSP polarization, the sapphire/PVNODC spectra have only two prominent vibration bands, the larger corresponding to the d^+ methylene symmetric vibration at 2845 cm^{-1} and the smaller to the d^- methylene asymmetric band at ∼2918 cm^{-1}.[7] In comparison, the dominant peak at the PVNODC/air interface is the symmetric methyl stretching vibration at 2875 cm^{-1}, with a smaller Fermi resonance peak also observed at 2935 cm^{-1}.[5−7] Our previous analysis indicated that the alkyl side chains of PVNODC at the PVNODC/air interface are ordered and in a predominantly all-trans conformation.[5]

In addition to the five peaks below 3000 cm^{-1}, spectra from the hPS/PVNODC interface (Figure 3) show two major peaks above 3000 cm^{-1} corresponding to the phenyl C−H stretching modes of hPS. The peak at 3024 cm^{-1} is assigned to ν20b phenyl stretching mode.[8,20−21] We assign the second peak at 3053 cm^{-1} to ν2 symmetric stretching vibration shown in Figure 2A. This assignment is lower than at the air interface.[8] The C−H stretching modes of phenyl rings are sensitive to their local environment as evident from the shift in the infrared and Raman ν2 peak in liquid toluene as compared to gaseous toluene.[22] Similar shifts are also observed for SFG spectra for PS in contact with sapphire and other substrates.[8,23] The presence of both the ν20b and ν2 peaks in the SSP spectrum is different from the predominance of the ν2 peak at the PS/air interface. In comparison, the spectra in the SSP and PPP for hPS/PVNODC interface above 3000 cm^{-1} are similar to those observed previously at the sapphire/PS interface.[8]

Orientation and Conformation at PS/PVNODC Interfaces. Spectra in Figure 3 were fit to eq 3, and the fits are shown in the figure as solid lines. These spectra (SSP, SPS, and PPP) were fit simultaneously, with A_q, Γ_q, ω_q, χ_{NR}, and φ allowed to vary to obtain the best fits, and the results are shown in Table 1. Insight into the orientation and conformation of the PVNODC comes primarily from the peaks associated with methyl and methylene functional groups. The methyl groups can be considered to belong to either the C_{3v} point group or the C_s point group due their attachment to the alkyl side chains. However, in the C_s point group the r^- asymmetric stretching vibration is split into two independent normal modes.[24] However, in SFG studies this splitting is either not observed or resolved, as is the case here.[5−7,17,24,25] Therefore, we choose the C_{3v} point group and make the simplifying assumption of free rotation of the methyl group about the group symmetry axis, treating the two asymmetric methyl stretching modes as being degenerate, leaving only one vibration band for the two r^- normal modes of vibration. In the case of phenyl vibrations, instead of five independent normal modes, we have only used the two dominant modes, ν2 and ν20b, present in the spectra to fit the data in Figure 3. Next, we determine the possible tilt angles for methyl, methylene, and phenyl groups using the data in Table 1.

Table 1: Line Fit Results for PS/PVNODC Interface Spectra in the SSP, SPS, and PPP Polarizations

peak assignment	frequency	Γ_q	A_q (ssp)	A_q (sps)	A_q (ppp)
d^+	2844.0	3.9 ± 1.1	−2.5 ± 0.1	0.1 ± 0.3	0.3 ± 0.5
r^+	2875.4	3.5 ± 0.4	2.0 ± 0.1	1.3 ± 0.1	2.3 ± 0.2
d^-	2921.0	7.2 ± 0.5	4.6 ± 0.1	4.8 ± 0.2	9.9 ± 0.2
r^{FR}	2933.7	9.2 ± 0.5	8.1 ± 0.2	3.9 ± 0.3	11.9 ± 0.3
r^-	2957.8	10.5 ± 0.6	2.3 ± 0.2	7.9 ± 0.2	14.5 ± 0.3
$\nu 20_b$	3024.0	7.3 ± 0.6	−2.2 ± 0.1	−3.5 ± 0.1	−7.9 ± 0.2
ν_2	3053.1	8.0 ± 2.1	−3.2 ± 0.1	−2.2 ± 0.2	−8.8 ± 0.3
ν_{7a}	3073.0	10.0 ± 1.7	1.5 ± 0.4		5.7 ± 1.1
χ_{nr}			0.2	0.30	0.3
ϕ			255	255	255

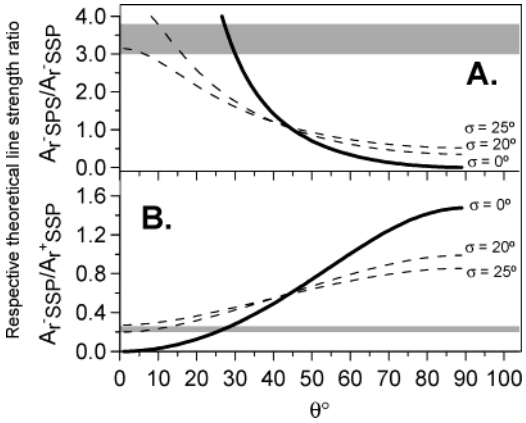

Figure 4. Theoretical ratios for the methyl peak line strength (A) (eq 6/eq 8) A_r^- SPS/A_r^- SSP and (B) (eq 7/eq 6) A_r^- SSP/A_r^+ SSP as a function of the tilt angle θ. The solid curves assume a δ-function angular distribution, and the dashed curves assume Gaussian distributions of width $\sigma = 20°$ and 25°, respectively. Horizontal bars represent the line strength ratios determined from experiments as shown in Table 1.

Orientation of Methyl Groups at the PS/PVNODC Interface. The methyl signal in the spectra can only come from the terminal group of the alkyl side chains in the carbamate polymer. The determination of tilt angles from eqs 6−9 requires the knowledge of β_{ccc}, β_{aac}, and β_{aca}. However, using the ratio of SPS to SSP r^- line strength (eqs 8 and 9), leads to cancellation of β_{aca}, and the ratio of $\chi_{eff,yzy}^{(2)}/\chi_{eff,yyz}^{(2)}$, as determined by Fresnel coefficients (eq 5), is ∼ 1 (see Supporting Information). The resulting theoretical SPS/SSP ratio of r^- line strengths A_r- SPS/A_r- SSP, with the assumption of a δ-function angular distribution, is plotted as a thick solid line in Figure 4A. The experimental value of the ratio of SPS to SSP r^- line strength for the PS/PVNODC interface from our fit in Table 1 is 3.4 ± 0.4 and is represented by the horizontal band shaded light gray in Figure 4A. The dashed lines in Figure 4A represent recalculation of the theoretical values by applying a Gaussian distribution of tilt angles given by eq 15 with width $\sigma = 20°$ and 25°, respectively. The intersection of the horizontal band with the solid line representing the δ-function distribution ($\sigma = 0°$) represents an upper bound of 30° for the methyl tilt angles.

(20) Varsanyi. G. *Vibrational Spectra of Benzene Derivatives*; Academic Press: New York, 1969.
(21) Sears, W. M.; Hunt, J. L.; Stevens, J. R. *J. Chem. Phys.* **1981**, *75*, 1589−1597.
(22) Schwab, A. D.; Gautam, K. S.; Yeganeh, M.; Dhinojwala, A. Manuscript in preparation.
(23) Wilson, P. T.; Richter, L. J.; Wallace, W. E.; Briggman, K. A.; Stephenson, J. C. *Chem. Phys. Lett.* **2002**, *363*, 161−168.
(24) Bell, G. R.; Bain, C. D.; Ward, R. N. *J. Chem. Soc., Faraday Trans.* **1996**, *92*, 515−523.
(25) Goates, S. R.; Shofield, D. A.; Bain, C. D. *Langmuir* **1999**, *15*, 1400−1409.

The intersection with the dashed curves show that the assumed Gaussian angular distribution must have a width σ below 25°.

We have also checked the orientation of the methyl groups using the ratio of r^-/r^+ line strengths in the SSP spectra. However, this requires independent knowledge of two ratios of methyl group hyperpolarizabilities.[5,17] The first ratio β_{aac}/β_{aca} can be estimated as -1.05 on the basis of a bond additivity model.[26] The second ratio of β_{aac}/β_{ccc} (R) is obtained from bond additivity models incorporating a theoretically determined Raman polarizability ratio for a single C−H bond as $R \sim 2.24$ and an experimentally determined value of 2.5.[14,27,28] For our analysis we use an intermediate value of $R = 2.37$. Tilt analysis with the r^+ mode introduces another important complication via the Fermi resonance, a combination band that represents an overtone of a methyl-bending mode and borrows the intensity from the r^+ symmetric stretching mode.[26] To account for the lost r^+ intensity borrowed through Fermi resonance, we have added the line strength of the r^{FR} peak to the line strength of the r^+ peak in our analysis.

The resulting theoretical ratio of the r^- line strength to the r^+ line strength A_{r^-}/A_{r^+} in SSP (eq 6/eq 8), with the assumption of a δ-function angular distribution, is plotted as a thin solid line in Figure 4B. The experimental value for the $A_{r^-}/(A_{r^+} + A_{r^{FR}})$ line strength ratio in the SSP polarization combination from our fit to the hPS/PVNODC interface in Table 1 is 0.23 ± 0.03 and is shown by the horizontal light gray bar in Figure 4B. The dotted lines represent recalculation of the theoretical ratio assuming a Gaussian distribution described by eq 15. Similar to the A_{r^-} SPS/A_{r^-} SSP ratio, the area where the light gray bar intersects the δ-function distribution curve provides an upper bound of 29° and again shows that the width of the assumed angular distribution σ must be less than 25°. For an all-trans alkyl chain this would correspond to the chain axis (ζ in Figure 2) tilted less than 20° with respect to the surface normal.

Conformation of PVNODC Alkyl Side Chains. The presence of a methylene signal in the SFG spectra can also be used to provide structural information on the PVNODC polymer at the interface. The methylene signals can originate from the methylene group in the polymer backbone as well as the alkyl side chains. Because of the presence of both methyl and methylene signals, we tentatively assign the methylene signals to the alkyl side chains. The similarity in the appearance of the methylene peak at the PVNODC/water interface below the side-chain melting temperature, where significant rearrangement of the backbone at the surface is not expected, supports this hypothesis.[29] SFG spectra from both PVNODC/air and PA-18/air interfaces do not show significant methylene peaks. It has been shown, by use of grazing angle X-ray diffraction, that the alkyl side chains at the air interface are crystalline at room temperature for PA-18.[30] The PVNODC side chains are also expected to be crystalline at room temperature on the basis of DSC measurements in the bulk. Therefore, the significantly larger methylene peaks observed for the hPS/PVNODC interface suggest that there must be more gauche defects and that the methyl groups of some of the alkyl chains are disordered at the interface.

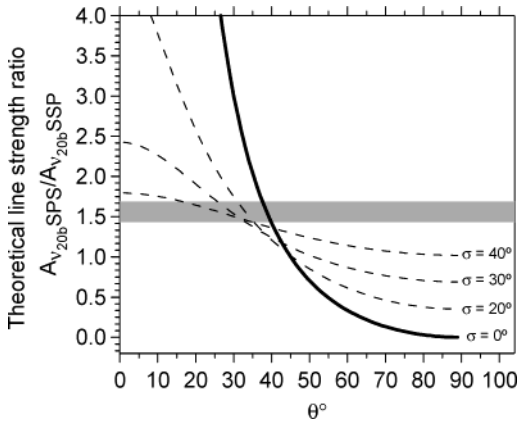

Figure 5. Ratios of $A_{\nu 20b}$ SPS/$A_{\nu 20b}$ SSP asymmetric line strengths as a function of tilt angle (θ) for molecules with C_{2v} point-group symmetry (eqs 10−13). The solid curve assumes a δ-function distribution of tilt angles, and the dashed curves assume Gaussian distributions with width $\sigma = 10°$, 20°, 30°, and 40°, respectively. Horizontal bars represent the experimental line strength ratios for the phenyl groups (Table 1).

Phenyl Group Orientation at the PS/PVNODC Interface. Analysis of the orientation of the phenyl groups can be conducted by use of eqs 12 and 13 and the assumption of a C_{2v} point group. Because of the ambiguity in the values for the hyperpolarizability ratio $R = \beta_{aac}/\beta_{ccc}$ ranging from 0.3 to 1, we have only used the analysis based on the ratio of ν20b line strength in SPS/SSP in Figure 5 to determine the tilt angles for the phenyl group.[22] On the basis of the SPS/SSP ν20b line strength ratio of 1.56 ± 0.13 from the fit in Table 1, represented in Figure 5 by the light gray horizontal bar labeled ν20b, the range of possible tilt angles includes all tilts below 40° when we account for the possibility of a Gaussian distribution as indicated by the dashed curves in Figure 5. Measurements from an alternate analysis to determine the tilt of the phenyl groups on measurements at the PS/Air interface yield a phenyl tilt of ~20°.[8] Thus, the phenyl groups at the PS/PVNODC interface are tilted at angles equal to or greater than those previously observed at the PS/air interface, similar to those observed at the sapphire/PS interface.[8]

B. PS/Alkyl Side-Chain Polymer Interfaces on Heating. The changes in SFG intensity for hPS and dPS in contact with PA-18 are shown in Figure 6. The spectra were acquired on the second SFG spectrometer described in part B of the Experimental Section. The system's greater infrared bandwidth results in lower peak resolution. However, it has a better signal-to-noise ratio and provides better sensitivity for the heating measurements. While the peaks do appear broadened by the convolution with the wider bandwidth infrared beam, the room-temperature spectra are fit with parameters similar to those described in the discussion above, and total methyl, methylene, and phenyl amplitudes are comparable within the estimated error. The peaks observed at 2880 and 2930 cm^{-1} in the SFG spectra in Figure 6 represent a convolution of the methyl and methylene peaks observed in the SSP spectra in Figure 3 discussed in part A. It is immediately clear that the spectral intensity of all peaks in the spectra from both hPS/PA-18 and dPS/PA-18 decrease with increasing temperature. There is an abrupt change in intensity at 43 °C, very close to the bulk

(26) Hirose, C.; Akamatsu, N.; Domen, K. *J. Chem. Phys.* **1992**, *96*, 997−1004.
(27) Gough, K. M. *J. Chem. Phys.* **1989**, *91*, 2424−2432.
(28) Oh-e, M.; Lvovsky, A. I.; Wei, X.; Shen, Y. R. *J. Chem. Phys.* **2000**, *113* (19), 8827−8832.
(29) Rangwalla, H.; Schwab, A. S.; Yeganeh, M. S.; Dhinojwala, A. *Langmuir* **2003** (submitted for publication).
(30) Gautam K. S.; Kumar, S. K.; Wermeille, D.; Robinson, D.; Dhinojwala, A. *Phys. Rev. Lett.* **2003**, *90*, 215501−1/5.

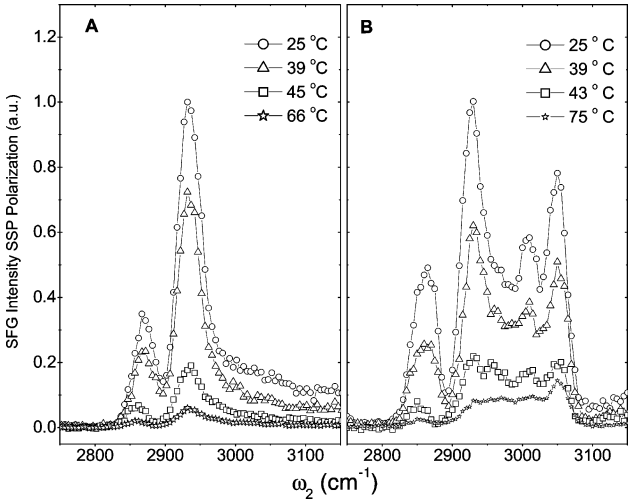

Figure 6. (A) Selected SFG spectra acquired at different temperatures for (A) dPS/PA-18 and (B) hPS/PA-18 interfaces. The incident angle was kept constant at $\phi_A \approx 8°$.

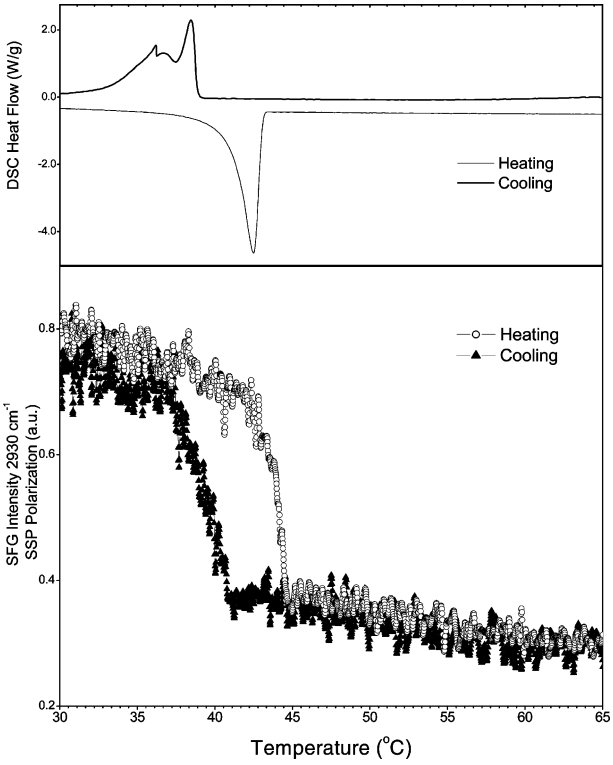

Figure 7. (Top panel) DSC heating and cooling scans at 0.5 °C/min for PA-18 (second heat and cooling cycle). (Bottom panel) SFG intensity from the 2930 cm^{-1} peak in the SSP polarization for dPS/PA-18 interface at an incident angle $\phi_A \approx 8°$ as the interface was heated and cooled at a rate of 0.5 °C/min.

melting temperature. Interestingly, the phenyl peaks also drop sharply at the same temperature as the methyl and methylene peaks, well below the bulk T_g of PS (bulk T_g for PS $\sim$ 100 °C).

To investigate the transition temperature in detail we have monitored the SFG intensity at 2930 cm^{-1} at a constant heating and cooling rate of 0.5 °C/min, as shown in Figure 7. For comparison we have also included the bulk transition temperatures in the heating and cooling cycle measured by DSC. A sharp drop in SFG intensity is observed at 43°; the midpoint of this drop corresponds to 43.5 °C, which is very close to the bulk melting temperature in the DSC trace. On cooling, the SFG

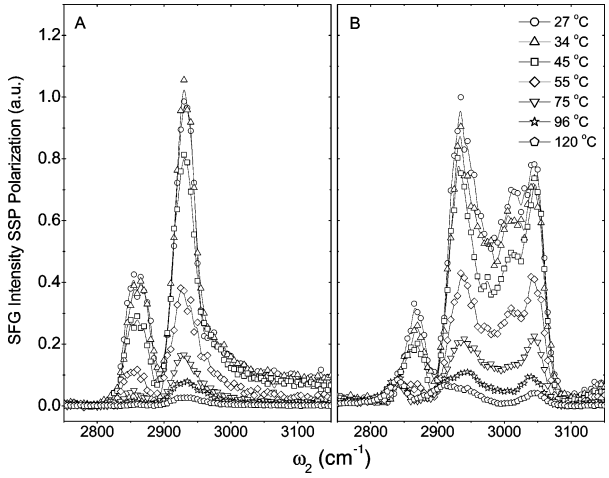

Figure 8. SFG spectra acquired at different temperatures and an incident angle $\phi_A \approx 8°$ from (A) dPS/PVNODC and (B) hPS/PVNODC interfaces.

intensity comes back to its original value with a 3−4 °C hysteresis. In fact, the decrease of the PS phenyl peak intensity on pace with the methyl and methylene intensity of PA-18 suggests the phenyl groups at the surface rearrange at the interface in response to the changes in the structure of the PA-18 side chains. One should bear in mind that NMR, neutron, and dielectric measurements have demonstrated bulk PS phenyl groups maintain significant mobility even below the bulk T_g.[31−33] Furthermore, also not clear is the degree of penetration of alkyl side chains within the PS phase at the interface and its influence on local T_g.

Interestingly, the single-step drop in SFG intensity from PA-18 near T_m at the dPS/PA-18 interface is in sharp contrast to the two-step behavior observed at the PA-18/air interface.[6] At the PA-18/air interface, the SFG, X-ray diffraction, and X-ray reflectivity measurements show that below T_m the surface alkyl side chains are crystalline and oriented almost normal to the surface.[6,30] On heating, two transitions are observed: the first 1−2 °C higher than the bulk melting temperature, T_m, and the second 10 °C above T_m. The X-ray reflectivity and SFG data suggest that the second transition is associated with disordering of the surface smecticlike state to an isotropic melt.[6,30] The driving force for maintaining an ordered surface layer has been attributed to the lower interfacial energy obtained due to the presence of ordered methyl groups in comparison to the methylene groups at the air interface.[6] When the strong driving force to minimize interfacial energy is removed by contacting PA-18 with hydrophilic sapphire or relatively less hydrophobic PS (as compared to the interface with air or a vacuum), only one transition is observed close to the bulk T_m.

Finally, we discuss the SSP SFG spectra from the hPS/PVNODC and dPS/PVNODC interfaces as a function of temperature, shown in Figure 8. It is immediately clear that the spectral intensity of all peaks in the spectra from both dPS/PVNODC and hPS/PVNODC decreases gradually, in contrast to the sharp drop observed for PA-18, as the temperature is raised. The contrast in the drops in SFG intensity between PVNODC and PA-18 is due to differences in bulk transitions

(31) Scheaefer, J.; Sefelk, M. D.; Stejskal, E. O.; McKay, R. A.; Dixon, T. W.; Cais, R. E. *Macromolecules* **1984**, *17*, 1107−1118.
(32) Khare, R.; Paulaitis, M. E. *Macromolecules* **1995**, *28*, 4495−4504.
(33) Kanaya, T.; Kawaguchi, T.; Kaji, K. *J. Chem. Phys.* **1996**, *104*, 3841−3850.

of these two polymers. PVNODC, in addition to having a side-chain crystalline phase, also exhibits a smectic liquid crystalline phase and shows three broad DSC peaks.[5] The first DSC peak is centered at 55 °C and corresponds to melting of the side chains to a smectic state. The second DSC peak is associated with transition changes in the interlayer spacing at 75 °C, and the third DSC peak at 93 °C is due to a transition from smectic to the isotropic state. Even though the SFG intensity gradually decreases upon heating, the surface alkyl chains are still ordered above T_m due to the presence of the bulk smectic phase. The methyl peak is reduced considerably only after the sample is heated above the smectic-to-isotropic transition temperature, 93 °C. Closer examination of the broad peak ~2870 cm^{-1} composed of convoluted r^+ and d^+ peaks reveals a shift to 2840−2850 cm^{-1} with increased temperature for both the hPS/PVNODC and dPS/PVNODC spectra. The difference in the strength of the emerging shifted methylene vibration for the hPS/PVNODC as compared to the dPS/PVNODC interface tentatively suggests that it originates from the methylene units of the hPS polymer backbone.

Similar to the behavior observed at the hPS/PA-18 interface, the drop in phenyl intensity observed at the hPS/PVNODC interface follows the gradual drop of the methyl and methylene signal with increasing temperature. This is in contrast to the observed behavior at PS/air and sapphire/PS interfaces, where we do not observe any significant changes in the SFG spectra on heating above the bulk T_g of PS.[8,34] Interestingly, for the hPS/PVNODC interface the ratio of ν20b peak to the ν2 peak is significantly different above 75 °C in comparison to that of the spectra below T_m and resembles the spectra observed at the PS/air interface above 3000 cm^{-1}. This suggests that the structure of the phenyl groups is similar to that at the PS/air interface above the smectic−isotropic transition temperature for PVNODC.

The presence of methylene peaks and a sharp order-to-disorder transition can be explained by the presence of heterogeneity either parallel or perpendicular to the interface. Heterogeneity parallel to the interface would imply crystalline domains consisting of all-trans alkyl side chains surrounded by grain boundaries with disordered alkyl side chains. On the other hand, heterogeneity perpendicular to the interface would imply disordered alkyl chains at the interface with a crystalline layer underneath. Molecular dynamics simulation and partial deuteration of comb polymers are in progress to elucidate these differences.

C. Structure and Adhesion. The SFG spectra and the analysis of methyl, methylene, and phenyl peaks indicate that the interface is relatively sharp and consistent with the expected good release properties of PVNODC films in coating applications.[2,3] However, the large methylene signal of the PVNODC side chains indicates the interface is not completely methyl-terminated and that side chains are relatively more disordered than those at the PVNODC/air interface.[5] To verify the good release properties, the bilayer samples were tested by a simple peel test described in part A of the Experimental Section. For all of the samples tested, failure consistently occurred at the PS/PVNODC interface, indicating it is much weaker than the PS/sapphire interface. This suggests little intermingling of PS chains and the alkyl side chains and that the interfacial interactions between these two polymers are weak.

5. Summary

In summary, this work leads to four salient observations. First, a strong methylene signal is observed, indicating the presence of gauche defects in the PVNODC and PA-18 polymers at interfaces with PS. Second, the terminal methyl groups of PVNODC are oriented very similarly to those at the air interface. Third, the methyl signals drop sharply near bulk T_m, indicating a sharp order-to-disorder transition at PS/PA-18 interfaces. Finally, the presence of both ν_2 and ν_{20b} vibrational modes suggests the orientation of phenyl groups is similar to that near a rigid sapphire substrate.

Acknowledgment. We gratefully acknowledge funding from NSF (Career Award to A.D.), 3M Corporation, and Petroleum Research Funds. We also thank Dr. Alexander D. Schwab for developing the SFG fitting program and for many helpful discussions.

Supporting Information Available: Relevant optical parameters as described in the text (PDF). This information is available free of charge via the Internet at http://pubs.acs.org.

JA035513V

(34) Schwab, A. D.; Dhinojwala, A. *Phys. Rev. E* **2003**, *67*, 021802−1/10.